3D Mouse Left Ventricle Reconstruction using Sparse MR Images with Arbitrary Orientations

Yang Yu[1], Jingjing Liu[1], Dimitris Metaxas[1], Leon Axel[2]

[1]Department of Computer Science, Rutgers University, Piscataway, NJ, USA
[2]Radiology Department, New York University, NY, USA

Abstract. This paper presents a framework for 3D left ventricle reconstruction using sparse magnetic resonance (MR) images with different orientations. Due to the inadequate inter-slice resolution, both short- and long-axis cardiac MR images are commonly acquired to reveal the left ventricle shape and motion. The contours in these images show different profiles of left ventricle and contain its essential shape information. In this paper, we propose a new deformable model to segment left ventricle on 2D slices with different orientations, and reconstruct its 3D model that matches all the contours in the images. An alternating optimization algorithm is proposed to efficiently solve the problem. The framework is applied on mouse cardiac MR data and shows promising results.

1 INTRODUCTION

In recent years, magnetic resonance imaging (MRI) is frequently used for the analysis of cardiac function. It enables the generation of 3D deformable models of the heart, from which accurate diagnostic information can be derived. However, it is hard to acquire high-resolution 3D cardiac MR images in animals due to the fast beating heart and the breathing, especially from the experimental small animals, like a mouse. The mouse heart is about 1000th the size of a human heart and beats much faster, at 400-600 beats per minute (bpm), than a human heart, with 60-80 bpm. Although currently available MRI instruments for mouse imaging operate at a higher magnetic field strength (4.7T or above) than clinical MRI scanners, they are still unable to provide adequate spatial resolution in 3D. In practice, only sparse good quality images on a few short- and long-axis slices are acquired to visualize the cardiac motion. They provide enough information for experts to visually analyze the cardiac motion, while it is still very challenging to reconstruct a 3D heart model based on these sparse slices [15].

Most of the previous work focuses on left ventricle reconstruction based on short-axis [9–11]. Since the short-axis images are parallel to each other, they are usually combined to a 3D volume. However, due to the limited number of slices, the inter-slice resolution is usually much lower than intra-slice directions. The distance between slices is about 10 times the pixel distance inside each slice. During the MR image acquisition, the long-axis images usually are first generated to localize the heart position, while they are rarely used for the segmentation for the left ventricle [5, 12]. These images have higher resolution in the long axis, which can help overcome the low inter-slice resolution on short-axis images. Therefore, we utilize both short- and long-axis MR

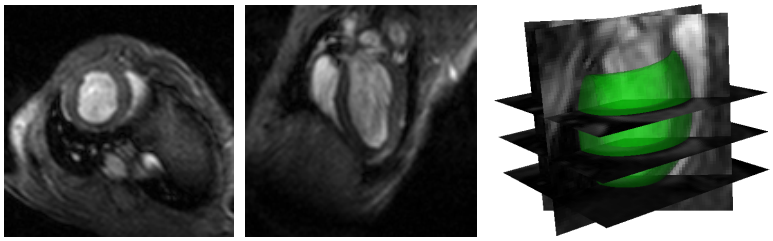

(a) Short axis image (b) Long axis image (c) 3D embedded view

Fig. 1: The mouse left ventricle has a ring shape on the short-axis images (a) and a U shape on the long-axis images (b). By mapping them to the 3D anatomic space, they intersect with the reconstructed left ventricle model exactly on the left ventricle boundaries (c).

images simultaneously in this work for 3D left ventricle reconstruction. Each image at different position provides different contours of the model. Meanwhile, the consistency among them improves the robustness of the reconstruction.

The short- and long-axis images are instances of the same volume of different orientations. Fradkin et al. [6] utilized their consistency to infer the short-axis image position based on the long-axis segmentation result. However, the spatial relationship is only used for initialization. The short-axis contours are then deformed independently. The contours after deformation may be inconsistent with the long-axis ones. Koikkalainen et al. [7] reconstructed a 3D heart model based on parallel MR images from the short and long axes. Different from usual long-axis slices, which are radially placed, they acquired parallel images in the long axis. The slices with different orientations are considered as volume data of the same region with different resolutions. A reference model is registered with them simultaneously to overcome the insufficient sampling for each single volume data. Since most long-axis images are not parallel in MR acquisition, their method will require on additional protocol for heart reconstruction. van Assen et al. [1] proposed a left ventricle reconstruction algorithm based on multiple shape priors. Based on active shape models (ASMs), they first build a point distribution model from training shapes, and then fit this model to all the 2D images to refine the segmentation. The images generate forces on the intersection of the 3D model with the corresponding 2D plans. Similarly, sparse shape composition [16] is used to represent shape models based on sparse reconstruction. The methods, like ASM, represent the shapes based on a large number of training samples, but the training shapes are not always available in clinical applications.

To address the limitations in previous efforts to incorporate 2D slices with arbitrary orientations for 3D left ventricle reconstruction, we introduce a new reconstruction framework. The main contributions of the work are as follows. First, all the slices are segmented simultaneously with a 3D left ventricle model. The 2D contours are just the projection of the model on the corresponding images, so we handle the inconsistency among all the contours, i.e., the short- and long-axis contours are not exactly intersected. Second, there are no restrictions on the position and orientation of each s-

lice. Any additional slice will help improve the segmentation accuracy and robustness. Third, only an elastic shape prior [4] is required in our framework. The reference shape can be generated with one sample data or built manually by expert without any sample. Different from the methods based on multiple shape priors, which ensure that the shape follows a point distribution model, we constrain the non-rigid deformation of the reference shape. The 3D shape regularization term is integrated into all the 2D image segmentations to form a unified problem, which is efficiently solved by our proposed alternating optimization algorithm.

2 METHODOLOGY

Given a group of 2D cardiac MR images I_i, which have known transformations T_i to the 3D anatomical coordinate system, we expect to reconstruct a 3D left ventricle shape model $T(S_{ref})$, where S_{ref} is a reference left ventricle model and T is a non-rigid transformation. The projection of the reconstructed model $T(S_{ref})$ onto image I_i is defined as $P_i(T(S_{ref}))$. It should match with the left ventricle area in the image. The fitness of the model to each image I_i is measured by the energy function E_{img}. Since the slices are sparse in the 3D volume, the reconstruction problem is under constrained with only the image information. Therefore, we further assume the model is deformed from the reference model S_{ref} with a smooth non-rigid deformation T. The model reconstruction is formulated as the following optimization problem:

$$\min_T \{\sum_i E_{img}(P_i(T(S_{ref})), I_i) + \gamma R(T)\} \tag{1}$$

where E_{img} is the energy term for the fitness to each image I_i, $R(T)$ is the regularization term for the deformation T and γ is a trade-off parameter.

The image energy term E_{img} is defined based on both the shape and appearance information. The conventional active contour models focus only on the boundaries of the models. They deform the contours to fit locations that have high probabilities to be boundaries. In our model, we also consider the appearance of the interior region. The appearance statistics are adaptively learned during the deformation. The model is updated based not only on the edge information, but also the region statistics to ensure the appearance consistency of the new territory. The region-based deformable model is defined based on free form deformation. Instead of deformable contours, the whole interior region is deformed to optimize both the edge and the region energy function:

$$E_{img} = E_{edg} + \mu E_{reg} \tag{2}$$

where E_{edg} is the edge energy term, E_{reg} is the region energy term and μ is a constant that balances the contributions from the two terms. In our formulation, we are able to omit the model smoothness term in 2D images since the whole model smoothness is regularized by the smooth non-rigid transformation of the 3D model.

The model is attracted to edge feature with high image gradient via the edge energy term E_{edg}. A distance map to the edge feature is built based on gradient vector field [14]. The edge force moves the contour to the minimum of the distance map. Therefore, the edge energy term E_{edg} is defined as:

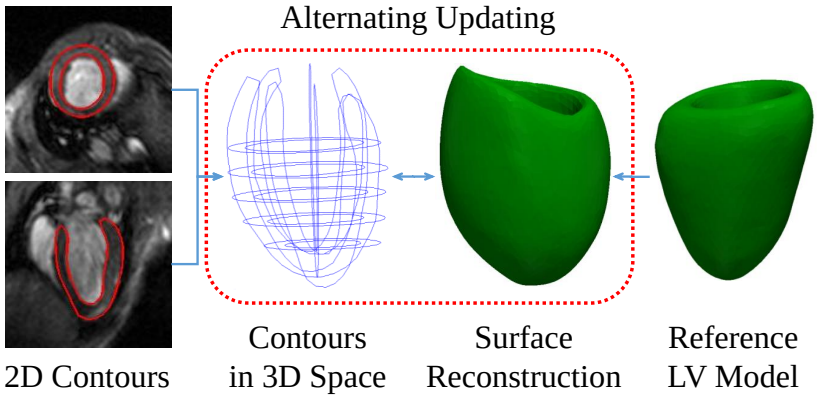

Fig. 2: The pipeline of our 3D left ventricle system. The 3D surface model is deformed from a reference model to fit 2D contours, while the 2D contours is constrained by both image cues and 3D model prior. They are updated alternatingly to reconstruct the left ventricle model.

$$E_{edg} = \int_C \Phi(\mathbf{x}) d\mathbf{x} \tag{3}$$

where C is the contour in a 2D image and Φ is the distance map function.

The probability of each pixel belonging to the model is defined based on the interior intensity distribution from last iteration. The region energy term deform the model toward areas with high probability. It is defined as:

$$E_{reg} = \int_R \log P(\mathbf{x}) d\mathbf{x} \tag{4}$$

where R is the interior region of the contour and P is the probability of each pixel as the interior region of the model.

The 2D contours are projections of one 3D left ventricle model to the corresponding images. Therefore, different from the 2D deformation regularization term in previous segmentation algorithms, we employ a 3D shape prior to constrain all the 2D segmentations simultaneously. The 3D model is defined based on the deformation of a reference left ventricle model $T(S_{ref})$. We regularize the non-rigid deformation T to ensure that the new model is still similar to the reference one. The smoothness of transformation T is defined as:

$$R(T) = \int_{\mathbb{R}^3} \frac{\tilde{T}(\tilde{\mathbf{x}})}{\tilde{G}(\tilde{\mathbf{x}})} d\tilde{\mathbf{x}} \tag{5}$$

where G is Gaussian kernel function and $\tilde{G}$ is its Fourier transform. Function $\tilde{T}$ indicates the Fourier transform of the deformation function T and $\tilde{\mathbf{x}}$ is a frequency domain variable. Gaussian kernel is used as a low-pass filter to regularize the high frequency part of the deformation and enforce the smoothness.

Algorithm 1 3D left ventricle reconstruction

Input: The sparse images I_i with arbitrary orientation, and the reference left ventricle model S_{ref}
Output: The data-specific 3D left ventricle model
Initialize the 2D contours C_i with graph cuts
repeat
  Transform the contours C_i to 3D anatomic space
  Deform the 3D reference model S_{ref} based on (7)
  Find the model-plane intersections $P_i(T(S_{ref}))$
  Deform the contours C_i based on (8)
until C_i and T converge.

2.1 Deformable Model Implementations

The image forces are only defined on the intersection of the model in each plane. They are not applied directly to the vertices of the model. Therefore, we introduce the contours of the left ventricle on the images C_i and reformulate the energy function as:

$$\min_{C_i,T}\{\sum_i [E_{img}(C_i,I_i)+\lambda D(C_i,P_i(T(S_{ref})))]+\gamma R(T)\} \tag{6}$$

where D is the distance between the contour C_i and the projection of the left ventricle model $P_i(T(S_{ref}))$. In this formulation, instead of deforming the reference model directly, the image forces only deform the 2D contours. Therefore, the whole energy function is separated into two parts. The 2D contours and the 3D model can be optimized alternatingly with Algorithm 1.

We initialize the 2D segmentation via graph cuts [2, 3]. It is very effective to generate a coarse segmentation, while it requires lots of interaction to refine the result. In our work, we use a two-stage segmentation for short-axis images based on its donut shape [13]. We use only a few strokes to indicate the blood pool. Then the left ventricle is automatically segmented with no further interaction. Furthermore, the long-axis images are also segmented via graph cuts, which initialized based on its relative position with short-axis images. The regional segmentation results on all the images are then translated into boundary ones and refined by Metamorphs [13].

The initial contours are first transformed to the 3D anatomic space. Then assuming the contours C_i are fixed, the reference left ventricle model is deformed to the contours. The energy function is reduced to:

$$\min_T\{\lambda\sum_i D(C_i,P_i(T(S_{ref})))+\gamma R(T)\} \tag{7}$$

We use coherent point drift [8] to optimize (7). The result model maintains the shape of the reference model, and balances the differences among the contours in different slices.

The deformed model $T(S_{ref})$ is then projected to the 2D spaces. We use them as shape priors and optimize the contours C_i. In this step, the energy function is independent for each slice:

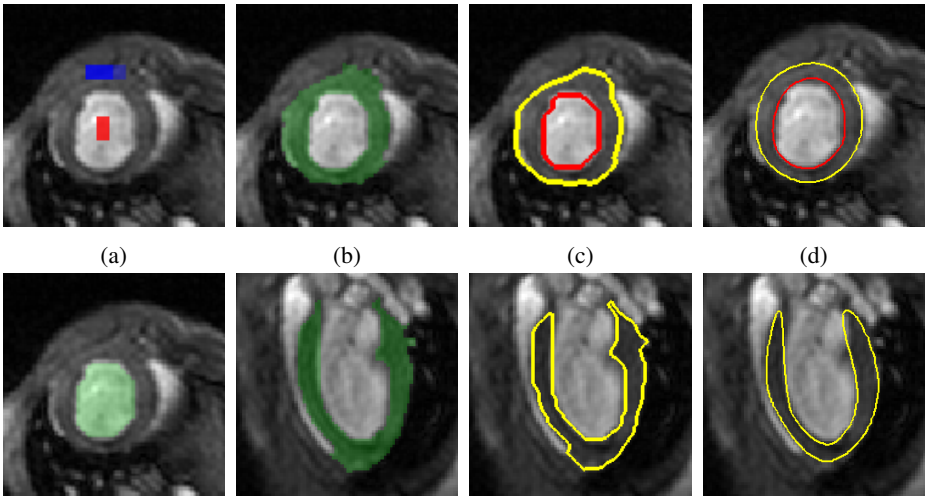

(a) (b) (c) (d)

(e) (f) (g) (h)

Fig. 3: (a) The initial label for graph cuts, (e) the blood pool segmentation result, (b, f) the left ventricle region (green) from graph cuts on both short- and long-axis images, (c, g) the boundaries based on graph cuts and (d, h) the finial result based on our framework.

$$\min_{C_i}\{E_{img}(C_i,I_i)+\lambda D(C_i,P_i(T(S_{ref})))\} \tag{8}$$

where the distance function D are defined by the distance maps of the model projection on the slices. This will make the contours more consistent with the left ventricle model.

During the alternating optimization, the parameter λ will increase to further enforce the consistency between the left ventricle model and all the contours. When $\lambda \to \infty$, the alternating algorithm (6) will converge to (1).

3 EXPERIMENTS

We test our reconstruction algorithm on mouse cardiac MR images. Sparse short- and long-axis images are acquired from the C57BL/6 mice. For each data, there are four to six short-axis slices that are parallel to each other with equal intervals, and four long-axis slices that are radially spaced every 45°. Their positions in the anatomic space are recorded during the acquisition.

We use a few strokes inside and outside the blood pool area, as shown in Fig. 3a, to initialize the segmentation, and get the blood pool area in Fig. 3e. This step is relatively stable due to the high intensity difference between the blood and heart wall. Then the region just outside the blood pool is set as the left ventricle. Graph cuts is used to produce a rough segmentation of the left ventricle on both short- and long-axis

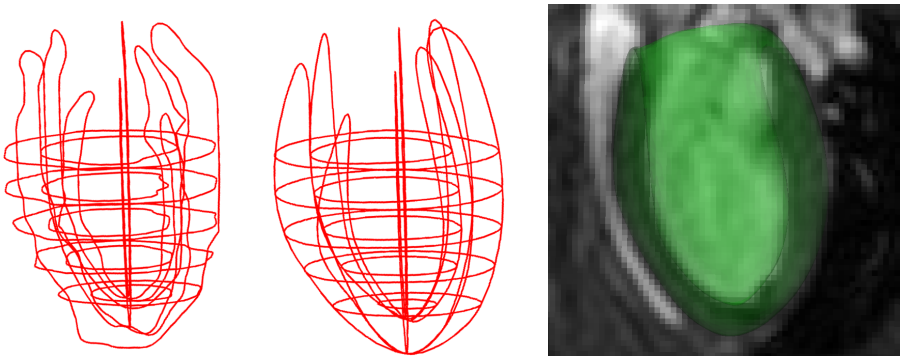

(a) Initial contours (b) Result contours (c) Result model

Fig. 4: (a) The initial 2D contours mapped onto 3D anatomic space, (b) the result contours after deformation based on our framework and (c) the resulted 3D model embedded onto a long-axis image.

images. The result of this step often leaks out to other tissues due to the similar intensity among them (Fig. 3b, f). It consequently affects the corresponding boundaries refined by Metamorphs, which cannot correct the region with heavy leak (Fig. 3c, g). Our proposed deformable model overcome these problems with 3D shape constraints. It achieves better segmentation result in 2D images (Fig. 3d, h).

We apply our alternating reconstruction algorithm to generate 3D left ventricle model based on the initial 2D contours. It is noticeable in Fig. 4a that the contours from the short- and long-axis images do not intersect with each other based on only 2D information. Our model introduces a 3D shape model to regularize all the contours. It improves the the 2D segmentation results on different slices (Fig. 3d, h). Meanwhile, different from the initial contours projected into anatomic space, the our results balance their differences and make them consistent with each other (Fig. 4b). The 3D left ventricle model is also constructed based on our model. It is embedded into a long axis image in Fig. 4c. The model is smooth and match left ventricle wall in the image.

4 CONCLUSIONS

We have presented a new framework for 3D left ventricle reconstruction using sparse short- and long-axis images based on only one shape prior. Less MR images are required to acquire by using our method. This is not only very important for mouse cardiac imaging, but also desired for human data acquisition, since it will reduce the potential risk of strong magnetic field and improve the patient's comfort. In the future, we will test our framework on human cardiac MR data. Meanwhile, we will introduce a left ventricle detection module to substitute graph cuts-based initialization and build a fully automatic system.

References

1. van Assen, H.C., Danilouchkine, M.G., Frangi, A.F., Ordás, S., Westenberg, J.J.M., Reiber, J.H.C., Lelieveldt, B.P.F.: SPASM: A 3D-ASM for segmentation of sparse and arbitrarily oriented cardiac MRI data. Medical Image Analysis 10(2), 286–303 (2006)
2. Boykov, Y., Veksler, O., Zabih, R.: Fast approximate energy minimization via graph cuts. IEEE Transactions on Pattern Analysis and Machine Intelligence 23(11), 1222–1239 (2001)
3. Boykov, Y., Jolly, M.P.: Interactive organ segmentation using graph cuts. In: Delp, S.L., DiGoia, A.M., Jaramaz, B. (eds.) Medical Image Computing and Computer-Assisted Intervention, Lecture Notes in Computer Science, vol. 1935, pp. 276–286. Springer Berlin Heidelberg (2000)
4. Chen, S., Cremers, D., Radke, R.J.: Image segmentation with one shape prior – A template-based formulation. Image and Vision Computing 30(12), 1032–1042 (2012)
5. Ciofolo, C., Fradkin, M.: Segmentation of pathologic hearts in long-axis late-enhancement MRI. In: Metaxas, D., Axel, L., Fichtinger, G., Székely, G. (eds.) Medical Image Computing and Computer-Assisted Intervention, Lecture Notes in Computer Science, vol. 5241, pp. 186–193. Springer Berlin Heidelberg (2008)
6. Fradkin, M., Ciofolo-Veit, C., Mory, B., Hautvast, G., Breeuwer, M.: Fully automatic segmentation of short and long axis cine cardiac MR. In: 12th Annual SCMR Scientific Sessions, Journal of Cardiovascular Magnetic Resonance, vol. 11 (2009)
7. Koikkalainen, J., Pollari, M., Lötjönen, J., Kivistö, S., Lauerma, K.: Segmentation of cardiac structures simultaneously from short- and long-axis MR images. In: Barillot, C., Haynor, D.R., Hellier, P. (eds.) Medical Image Computing and Computer-Assisted Intervention, Lecture Notes in Computer Science, vol. 3216, pp. 427–434. Springer Berlin Heidelberg (2004)
8. Myronenko, A., Song, X.: Point set registration: Coherent point drift. IEEE Transactions on Pattern Analysis and Machine Intelligence 32(12), 2262–2275 (2010)
9. Petitjean, C., Dacher, J.N.: A review of segmentation methods in short axis cardiac MR images. Medical Image Analysis 15(2), 169–184 (2011)
10. Radau, P., Lu, Y., Connelly, K., Paul, G., Dick, A., Wright, G.: Evaluation framework for algorithms segmenting short axis cardiac MRI. MICCAI Workshop: Cardiac MR Left Ventricle Segmentation Challenge (2009)
11. Suri, J.S.: Computer vision, pattern recognition and image processing in left ventricle segmentation: The last 50 years. Pattern Analysis & Applications 3(3), 209–242 (2000)
12. Üzümcü, M., van der Geest, R.J., Sonka, M., Lamb, H.J., Reiber, J.H.C., Lelieveldt, B.P.F.: Multiview active appearance models for simultaneous segmentation of cardiac 2- and 4-chamber long-axis magnetic resonance images. Investigative Radiology 40(4), 195–203 (2005)
13. Uzunbas, M.G., Zhang, S., Pohl, K.M., Metaxas, D., Axel, L.: Segmentation of myocardium using deformable regions and graph cuts. In: International Symposium on Biomedical Imaging: From Nano to Macro. pp. 254–257 (2012)
14. Xu, C., Prince, J.L.: Snakes, shapes, and gradient vector flow. IEEE Transactions on Signal Processing 7(3), 359–369 (1998)
15. Yu, Y., Zhang, S., Li, K., Metaxas, D., Axel, L.: Deformable models with sparsity constraints for cardiac motion analysis. Medical Image Analysis 18(6), 927–937 (2014)
16. Zhang, S., Zhan, Y., Dewan, M., Huang, J., Metaxas, D.N., Zhou, X.S.: Towards robust and effective shape modeling: Sparse shape composition. Medical Image Analysis 16(1), 265–277 (2012)